

05,13

Control of band gap's in a permalloy Structure by changing the meander profile

© Yu.A. Gubanova, V.A. Gubanov, N. Noginova, A.V. Sadovnikov

Chernyshevsky Saratov National Research State University,
Saratov, Russia

E-mail: yulya29022095@gmail.com

Received April 29, 2022

Revised April 29, 2022

Accepted May 12, 2022

Control modes of band gap in meander-shaped permalloy (*NiFe*) thin films have been investigated by the method of micromagnetic modeling. The electrodynamic problem is considered by the finite element method and the dispersion characteristics of spin waves are obtained when the geometrical parameters of the meander are changed. The character of changes in the frequency ranges of the Bragg band gaps depending on the meander profile has been investigated. The results can be used to create devices for microwave signal processing, microwave filters and systems with spatio-temporal division of the signal.

Keywords: spin waves, magnonics, meander structures, magnon crystal.

DOI: 10.21883/PSS.2022.09.54162.15HH

1. Introduction

Development of methods for manufacturing nanoscale structures and controlled metamaterials based on them allows for creating a new class of composite materials whose properties can be controlled by changing the geometric parameters of the structures [1]. Using the method of forming magnetic films on corrugated substrates, it is possible to design magnonic-crystalline structures with predetermined properties [2–5]. The magnonic analogue of photonic crystals is a periodic structure made of a material in which spin waves (SWs) can propagate to a sufficient distance [6]. Such structures are called magnonic crystals (MCs) and are in fact a magnetic metamaterial with periodically changing parameters, which demonstrates the control of the SW delay, while the analysis of the dispersion characteristic of such structures allows us to state that in the SW spectrum one can identify periodically alternating frequency intervals in which propagation of SW (passbands) is observed, and frequency regions in which SW propagation does not occur, due to additional attenuation resulting from Bragg interference of the incident and reflected waves. The formation of such band gaps in the magnon spectrum enables to use MCs as filters for a signal encoded as the amplitude and phase of SW. The study of MC with different periodicity in one and two dimensions [7,8] has led to the development of the field of magnonics [9], in which the transport properties of spin-polarized electrons are not used, and information is transferred by signal transmission using SW [10]. This approach implements a number of signal processing functional blocks with low power consumption and possible compatibility with semiconductor electronic circuits.

In this article, we consider a magnon-crystalline structure formed by meander-like films, which consist of ferromagnetic nanosized segments located perpendicular to each other, while in each section the mode of propagation of surface magnetostatic spin waves is carried out, which allows the signal to propagate without significant losses in the junction region [11]. This approach enables to avoid the limitations associated with attempts to control SW [12,13], which are difficult to implement using plane magnetized films due to the anisotropic dispersion of SW, which depends on relative orientation of magnetization and wave vector. Using the micromagnetic modeling method based on the solution of the Maxwell equation, the spectrum of eigenmodes and the profiles of the magnetization distribution in a primitive cell, considered meander structure, are constructed, the possibility of controlling the band gaps of spin waves in a meander structure is shown.

2. Studied structures and numerical modelling

Figure 1, *a* shows the studied meander waveguide made of permalloy *NiFe*. Figure 1, *b* shows a segment of a periodic 3D-magnon structure in cross section used to simulate a meander structure with the following parameters: modulation period $L = 740$ nm, lower horizontal section height $m_1 = 50$ nm, upper horizontal section height $m_2 = 50$ nm, vertical section thickness $m_3 = 50$ nm, drop height $p = 120$ nm. The direction of the external magnetic field was along the Oz axis.

Numerical simulation was carried out by solving the system of Maxwell equations using the finite element method [14,15] in the COMSOL Multiphysics software

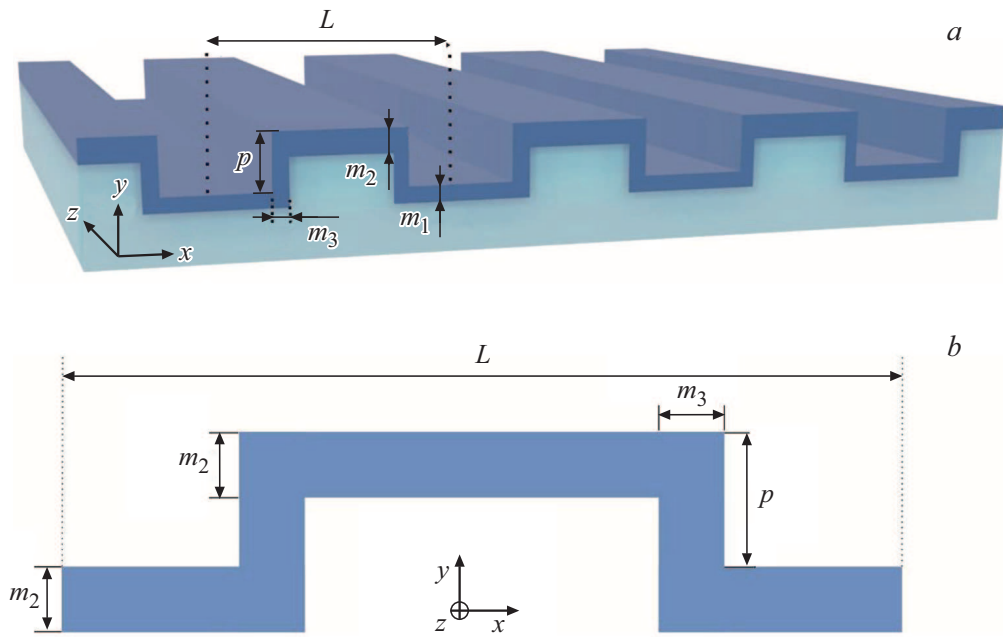


Figure 1. Images of the studied structure (a). A primitive cell used to model a meander pattern with dimensions (b).

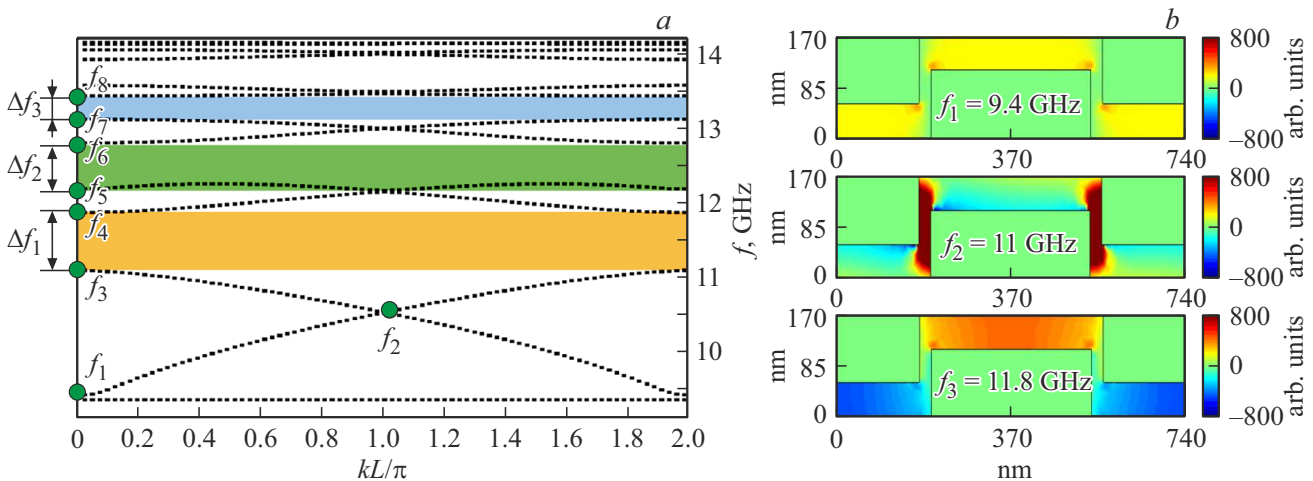


Figure 2. Dispersion characteristic, for a permalloy structure (a), spatial distribution of frequency modes of dynamic magnetization m_y (b).

product. The dispersion characteristics were calculated taking into account that the components of the electromagnetic field depended on the frequency according to the harmonic law. The equation for the electric field strength vector \mathbf{E} had the following form:

$$\nabla \times (\hat{\mu}^{-1} \nabla \times E) - k^2 \epsilon E = 0,$$

where $k = \omega/c$ is wave number in vacuum, $\omega = 2\pi/f$ is circular frequency, f is electromagnetic wave frequency, ϵ is effective value of permittivity. In this case, the magnetic permeability tensor for tangential magnetization

has the form

$$\hat{\mu} = \begin{vmatrix} 1 & 0 & 0 \\ 0 & \mu(f) & i\mu_a(f) \\ 0 & i\mu_a(f) & \mu(f) \end{vmatrix},$$

$$\mu(f) = \frac{-f_H(f_n + f_M) - f^2}{f_H^2 - f^2},$$

$$\mu_a(f) = \frac{f_M f}{f_H^2 - f^2},$$

where $f_M = \gamma 4\pi M_0$, $f_M = \gamma H_{in}(x)$, γ — gyromagnetic ratio. It should be noted that this method enables to

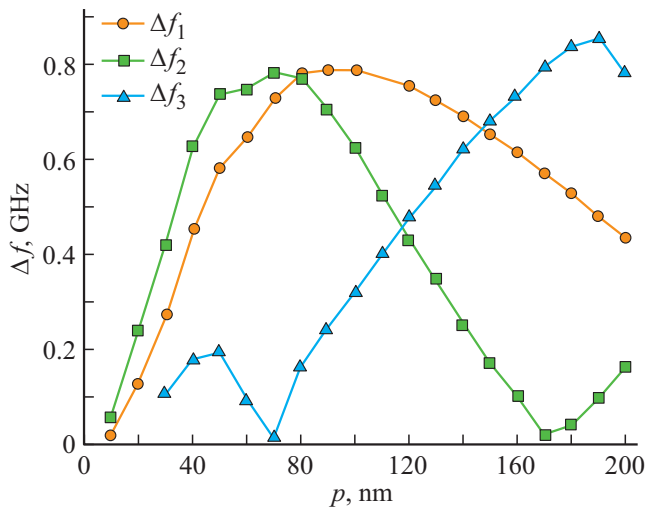


Figure 3. Dependence of the frequency ranges of the Bragg band gaps on the change in the drop height p .

make a calculation taking into account the heterogeneous distribution of the internal magnetic field $H_{\text{int}}(x)$.

As a result of numerical simulation, dispersion characteristics for direct and counterpropagating waves were obtained (Fig. 2, *a*). On the dispersion characteristic, one can also see the frequency ranges of the Bragg band gaps, in which spin waves do not propagate. The frequency band gap is of greatest importance for low frequency modes. It can be seen that in the frequency range from $f_1 = 9.4$ GHz to $f_3 = 11.8$ GHz, the first band gap does not form in the SW spectrum (near the wave number $k \sim k_B = \pi/L$), which is a consequence of the symmetry of the „sliding plane“ type for the structure under consideration. The color in Fig. 2, *a* denotes the frequency ranges of the Bragg band gaps: for waves with a wave number near $k \sim 2k_B$, the band gap formed (highlighted in orange in Fig. 2, *a*) Δf_1 is the largest and low-frequency and high-frequency boundaries for it are denoted as f_3 and $-f_4$, respectively. The next band gap is

formed for SW with a wave number near $k \sim 4k_B$ (green color in Fig. 2, *a*), its width is denoted by Δf_2 and cutoff frequencies — using symbols f_5-f_6 . For the stopband zone for SW with a wave number near $k \sim 6k_B$ (blue color in Fig. 2, *a*), the designation Δf_3 is introduced and cutoff frequencies are marked as f_7 and f_8 .

For spin wave modes propagating in a meander structure at frequencies f_1, f_2 and f_3 , the spatial distributions of the dynamic magnetization component m_y were calculated and plotted (Fig. 2, *b*). Since the lattice cell of the structure has a mirror symmetry about the vertical axis y , the spatial distributions for standing spin waves and Bloch waves in the primitive cell will also have this type of symmetry. The mode profiles at the edges of the band gaps correspond to standing waves with zero group velocity and the same Bloch wave number $k = 2\pi m/L$, $m = \pm 1, \pm 2$ in the periodic meander structure. These stationary waves are formed by successive reflections of propagating waves when the Bragg condition is satisfied. Symmetric mode profiles alternate with antisymmetric ones along with a monotonic increase in frequency at $k = 2\pi m/L$, $m = \pm 1, \pm 2$, and at $k = 2\pi m/L$, $m = \pm 1, \pm 2$. The mode profile undergoes smooth transition from the top of one open band gap to the bottom of the next band gap in order.

To analyze the influence of a change in the thickness of the vertical sections m_3 on the nature of the dispersion characteristic, the value of m_3 was taken to be 25 nm. As a result, it was revealed that at $k = 1$ the Bragg band gap appears in the frequency range Δf_0 from f_{21} to f_{22} .

Fig. 3 shows the dependence of the width of the frequency stopband zone on the meander drop p parameter for the first three frequency bands $\Delta f_1, \Delta f_2$ and Δf_3 with circles, squares and triangles, respectively. The drop parameter p varied in the range from 10 to 200 nm. The thickness of the ferromagnetic layer in the vertical section was $m_3 = 25$ nm. When the difference is $p = 75$ nm, the value of the frequency range of the first stopband zone, for waves with a wave number near $k \sim 2k_B$, is maximum and amounts to 0.8 GHz. In this case, for SW with a wave

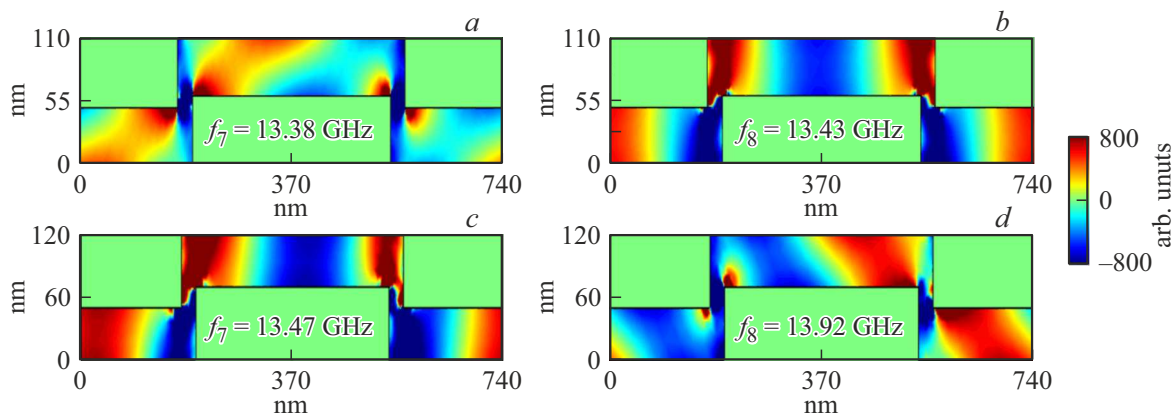


Figure 4. Spatial distributions of frequency modes of dynamic magnetization m_y in the frequency range Δf_3 : $p = 60$ nm at frequency $f_7 = 13.38$ GHz (*a*), $p = 60$ nm at frequency $f_8 = 13.43$ GHz (*b*), $p = 70$ nm at frequency $f_7 = 13.47$ GHz (*c*), $p = 70$ nm at frequency $f_8 = 13.47$ GHz (*d*).

number near $k \sim 6k_B$, the maximum value of the width of the stopband frequency zone is observed at approximately the same values of the drop parameter $p \sim 100$ nm. For SW with a wave number near $k \sim 4k_B$ at values of the parameter p in this range, the stopband zone value is minimal and reaches zero at $p = 70$ nm.

The case when the width of the third stopband frequency zone Δf_3 decreases in the drop height range of $60 < p < 80$ nm is associated with a change in the spatial distribution of the dynamic magnetization component m_y for the third wave mode. Fig. 4 shows the spatial distributions of the m_y component for the cases of $p = 60$ nm and $p = 70$ nm drop value variation in the frequency range Δf_3 , where f_7 is low-frequency boundary, f_8 is high-frequency boundary of the frequency range. It can be seen that at $p = 60$ nm at the frequency $f_7 = 13.38$ GHz (Fig. 4, *a*), in the Δf_3 region there is no phase change in the vertical section; at the frequency $f_8 = 13.43$ GHz (Fig. 4, *b*) in the vertical section, the phase changes by 180 degrees, respectively, with an increase in the parameter p the nature of the phase change changes at $p = 70$ nm at the frequency $f_7 = 13.47$ GHz (Fig. 4, *c*), in the Δf_3 region the phase reverses in the vertical section, at the frequency of $f_8 = 13.92$ GHz (Fig. 4, *d*) the phase changes slightly.

This means that near these values of the parameter p one can observe the closing of the Δf_3 band gap. By varying the depth of the meander modulation, it is possible to control the width of the stopband frequency zone in the spectrum of spin waves propagating in a meander structure, which can be used in the development and manufacture of microwave filters based on nanoscale magnon-crystalline structures made in the form of meander ferromagnetic films.

3. Conclusion

Thus, using the method of numerical simulation, we have studied the regimes of band gap control in the spectra of spin waves propagating in a periodic permalloy structure with a meander profile. The possibility of changing the Bragg band gap with a change in the parameters of the structure profile is demonstrated, and it is shown that, in contrast to the usual magnon-crystalline structure, in the considered meander structure with period L , band gaps are formed for spin waves, the wave number of which is determined from the equation $k = m^* \pi / L$, where m is an even number. In this case, the maximum value for the width of the first and second stopband zones is achieved for the drop parameter in the meander structure of $75 < p < 100$ nm, while the third stopband zone has the smallest width. The results obtained may be of interest for the development of controlled metasurfaces based on magnetic metamaterials. Meander magnonic structures can be used in the development and manufacture of microwave filters based on nanosized magnonic crystal structures.

Funding

The study was performed with the support of the Ministry of Education and Science of Russia under the Government Task (project No. FSRR-2020-0005).

Conflict of interest

The authors declare that they have no conflict of interest.

References

- [1] M.A. Noginov, V.A. Podolskiy. *Tutorials in Metamaterials*. CRC Press **308** (2011).
- [2] N. Noginova, V. Gubanov, M. Shahabuddin, Y. Gubanova, S. Nesbit, V.V. Demidov, A.V. Sadovnikov. *Appl. Magn. Res.* **52**, 7, 749 (2021).
- [3] A.V. Sadovnikov, G. Talmelli, G. Gubbiotti, E.N. Beginin, S. Sheshukova, S.A. Nikitov, C. Adelman, F. Ciubotaru. *J. Magn. Magn. Mater.* **544** (2022).
- [4] A.V. Chumak, P. Kabos, M. Wu, C. Abert, C. Adelman, A. Adeyeye, X. Zhang. *arXiv preprint arXiv*, 2111.00365 (2021).
- [5] E.Y. Vedmedenko, R.K. Kawakami, D.D. Sheka, P. Gambardella, A. Kirilyuk, A. Hirohata, A. Berger. *J. Physics D* **53**, 45, 453001 (2020).
- [6] M. Krawczyk, H. Puzskarski. *Appl. Mang. arXiv preprint cond-mat/0504073* (2005).
- [7] S.A. Nikitov, Ph. Tailhades, C.S. Tsai. *J. Magn. Mater.* **236**, 320 (2001).
- [8] S.A. Nikitov, A.R. Safin, D.V. Kalyabin, A.V. Sadovnikov, E.N. Beginin, M.V. Logunov, M.A. Morozova, S.A. Odintsov, S.A. Osokin, A.Yu. Sharaevskaya, Yu.P. Sharaevsky, A.I. Kirilyuk. *UFN*, **190**, 1009 (2020) (in Russian).
- [9] A.V. Chumak, A.A. Serga, B. Hillebrands. *J. Phys. D* **50**, 244001 (2017).
- [10] D.A. Allwood, G. Xiong, C.C. Faulkner, D. Atkinson, D. Petit, R.P. Cowburn. *Science* **309**, 5741, 1688 (2005).
- [11] K. Wagner, A. Kákay, K. Schultheiss, A. Henschke, T. Sebastian, H. Schultheiss. *Nature Nanotechnol.* **11**, 5, 432 (2016).
- [12] K. Vogt, F.Y. Fradin, J.E. Pearson, T. Sebastian, S.D. Bader, B. Hillebrands, A. Hoffmann, H. Schultheiss. *Nature Commun.* **5**, 3727 (2014).
- [13] J. Stigloher, M. Decker, H.S. Körner, K. Tanabe, T. Moriyama, T. Taniguchi, H. Hata, M. Madami, G. Gubbiotti, K. Kobayashi, T. Ono, C.H. Back. *Phys. Rev. Lett.* **117**, 037204 (2016).
- [14] A.G. Rozhnev. *Izv. vuzov. Prikladnaya nelineynaya dinamika*, **20**, 1, 143 (2012) (in Russian).
- [15] A.D. Vasil'ev, A.B. Manenkov. *Izv. vuzov. Radiofizika*, **30**, 3, 405 (1987) (in Russian).